Contribution from the J. Heyrovský Institute of Physical Chemistry and Electrochemistry, Czechoslovak Academy of Sciences, Dolejškova 3, 182 23 Prague 8, Czechoslovakia

Redox Properties of $[Mn(CO)_3(DBCat)]^-$ (DBCat = 3,5-Di-*tert*-butylcatecholate): Formation and Characterization of a Four-Membered Redox Series†

František Hartl and Antonín Vlček, Jr.*

Received November 19, 1990

The $[Mn(CO)_3$(3,5-di-*tert*-butylcatecholate)$]^-$ complex undergoes a metal-localized one-electron reduction ($E_{1/2}$ = −2.39 V vs Fc/Fc^+ in THF) and two successive one-electron oxidations ($E_{1/2}$ = −0.70, +0.23 V vs Fc/Fc^+ in THF) that are ligand localized. All redox steps are electrochemically reversible or quasireversible. The oxidations are followed by rapid coordination of a sixth ligand, i.e. THF, PPh_3, or CO in CO-saturated CH_2Cl_2 solution. In argon-saturated CH_2Cl_2, a CO ligand disproportionation of the oxidation products takes place. In effect, the existence of a four-membered redox series was established: $[Mn(CO)_3(L)$(quinone)$]^+$, $[Mn(CO)_3(L)$(semiquinone)$]$, $[Mn(CO)_3$(catecholate)$]^-$, and $[Mn(CO)_3$(catecholate)$]^{2-}$; L = CO, THF, or PPh_3. The spectral properties (EPR, IR, and UV-vis) of the neutral, monoanionic, and dianionic species are compared. The EPR spectra of the ligand- and metal-localized radicals $[Mn(CO)_3(L)$(semiquinone)$]$ and $[Mn(CO)_3$(catecholate)$]^{2-}$ are markedly different: a_{Mn} = 3.7 G (L = THF), 6.9 G (L = CO), 9.9 G (L = PPh_3); a_{Mn} = 53.4 G. The IR ν(CO) frequencies significantly increase from the dianion to the neutral species, reflecting the change in the Mn oxidation state in the mono-/dianion couple and the decrease in π-donation upon the oxidation of the catecholate to the semiquinone radical-anionic ligand.

Introduction

Dioxolene ligands (i.e. catecholate dianions and their oxidation products: semiquinone radical-anions and *o*-quinones)[1] are typical noninnocent ligands. Their redox properties are retained, albeit modified, upon their coordination in transition-metal complexes. As a consequence, the electrochemical behavior of complexes containing dioxolene ligands is rather intriguing.[2-18] Two one-electron redox steps per each dioxolene ligand are, in principle, observable. Dioxolene-localized electron-transfer steps may be accompanied by metal-localized oxidations and/or reductions that may occur at more positive and/or more negative potentials, respectively. The usual picture of the electrochemistry of metal–dioxolene complexes thus consists of a set of dioxolene-localized one-electron steps flanked by the metal-localized ones. Metal–dioxolene bonding seems not to be extensively delocalized,[3] so the oxidation-state concept appears generally appropriate[2,3,6,10] and the assignment of the localization of individual redox steps either to the metal atom or to the dioxolene ligand is usually valid. Dioxolene complexes of Ru and Os appear[2,6,10] to be the only exceptions because of more extensive delocalization caused by close energetic proximity between the metal d orbitals and the dioxolene π^* level.[6] In this respect, the dioxolene complexes are different from their dithiolene counterparts, whose redox chemistry is best described by a completely delocalized model.[19-21]

Although most dioxolene-localized redox processes are chemically fully reversible, slow homogeneous reactions following the electron-transfer steps were observed in some cases.[4,11,13,14,17,18] Generally, Cat-type ligands strongly stabilize metals in high oxidation states.[3,13,14,18] The donor ability of dioxolenes decreases in the order Cat > SQ > Q.[3] Therefore, the Cat/SQ couple may be expected to exhibit some chemical irreversibility in complexes of high-valent metals, as was observed e.g. for Mo(VI)[13,14] or Re(VI).[18] The SQ/Q couple was found not to be completely chemically reversible, even in some complexes of Co(III),[11] Cr(III),[4] or Ni(II).[17] However, the nature of the followup chemical reactions has seldom been studied in detail.

Recently, we synthesized and characterized a $[Mn(CO)_3$(DBCat)$]^-$ complex[22] that exhibits rather unusual properties: An electron-rich DBCat ligand is bound to a low-valent formally d^6-Mn(I) atom in a five-coordinate environment. Although this formally 16-electron complex is coordinatively unsaturated, it does not exhibit any tendency to add a sixth ligand.[22] The oxidation states of Mn and the DBDiox ligand were clearly assigned on the basis of structural and spectroscopic (IR, ^1H NMR, ^{13}C NMR, and UV-vis) properties. However, it is of interest to examine the validity of the oxidation-state concept in this complex from the electrochemical point of view. Because of its coordinative unsaturation, $[Mn(CO)_3(DBCat)]^-$ is suitable for investigation of the dependence of chemical and spectroscopic properties on the oxidation state of the DBDiox ligand and central Mn atom. The results of an electrochemical and spectroelectrochemical study on $[Mn(CO)_3(DBCat)]^-$ are reported herein.

Results

A. Reduction. Electrochemical reduction of $Bu_4N[Mn(CO)_3(DBCat)]$ in a THF solution (Figure 1, peak A) occurs at $E_{1/2}$ = −2.39 V (vs Fc/Fc^+)[23] in a single diffusion-controlled[24]

† Dedicated to Prof. Dr. Kurt Schaffner on the occasion of his 60th birthday.

(1) The term "dioxolene" (Diox) is used for ligands derived from 1,2-dioxobenzene irrespective of its oxidation state,[2] i.e. the catecholate dianion (Cat), the semiquinone radical anion (SQ), or *o*-quinone (Q), without specifying substituents on the benzene ring. The individual oxidation states of 3,5-di-*tert*-butyl-1,2-dioxobenzene (DBDiox) are in this study denoted DBCat, DBSQ, and DBQ.

(2) Lever, A. B. P.; Auburn, P. R.; Dodsworth, E. S.; Haga, M.; Liu, W.; Melnik, M.; Nevin, W. A. *J. Am. Chem. Soc.* **1988**, *110*, 8076.
(3) Pierpont, C. G.; Buchanan, R. M. *Coord. Chem. Rev.* **1981**, *38*, 45.
(4) Downs, H. H.; Buchanan, R. M.; Pierpont, C. G. *Inorg. Chem.* **1979**, *18*, 1736.
(5) Sofen, S. R.; Ware, D. C.; Cooper, S. R.; Raymond, K. N. *Inorg. Chem.* **1979**, *18*, 234.
(6) Bhattacharya, S.; Boone, S. R.; Fox, G. A.; Pierpont, C. G. *J. Am. Chem. Soc.* **1990**, *112*, 1088.
(7) Buchanan, R. M.; Claflin, J.; Pierpont, C. G. *Inorg. Chem.* **1983**, *22*, 2552.
(8) Cass. M. E.; Gordon, N. R.; Pierpont, C. G. *Inorg. Chem.* **1986**, *25*, 3962.
(9) deLearie, L. A.; Pierpont, C. G. *J. Am. Chem. Soc.* **1987**, *109*, 7031.
(10) Haga, M.; Dodsworth, E. S.; Lever, A. B. P. *Inorg. Chem.* **1986**, *25*, 447.
(11) Bianchini, C.; Masi, D.; Mealli, C.; Meli, A.; Martini, G.; Laschi, F.; Zanello, P. *Inorg. Chem.* **1987**, *26*, 3683.
(12) Bradbury, J. R.; Schultz, F. A. *Inorg. Chem.* **1986**, *25*, 4408.
(13) Bradbury, J. R.; Schultz, F. A. *Inorg. Chem.* **1986**, *25*, 4416.
(14) Gheller, S. F.; Newton, W. E.; deMajid, L. P.; Bradbury, J. R.; Schultz, F. A. *Inorg. Chem.* **1988**, *27*, 359.
(15) Girgis, A. Y.; Sohn, Y. S.; Balch, A. L. *Inorg. Chem.* **1975**, *14*, 2327.
(16) Wicklund, P. A.; Beckmann, L. S.; Brown, D. G. *Inorg. Chem.* **1976**, *15*, 1996.
(17) Benelli, C.; Dei, A.; Gateschi, D.; Pardi, L. *Inorg. Chem.* **1988**, *27*, 2831.
(18) deLearie, L. A.; Haltiwanger, R. C.; Pierpont, C. G. *Inorg. Chem.* **1987**, *26*, 817.
(19) McCleverty, J. A. *Prog. Inorg. Chem.* **1968**, *10*, 49.
(20) Schranzer, G. N. *Acc. Chem. Res.* **1969**, *2*, 72.
(21) Cleverty, J. A. *Reactions of Molecules at Electrodes*; Hush, N. S., Ed.; Wiley: London, 1971; p 403.
(22) Hartl, F.; Vlček, A., Jr.; deLearie, L. A.; Pierpont, C. G. *Inorg. Chem.* **1990**, *29*, 1073.
(23) Gagné, R. R.; Koval, C. A.; Lisensky, C. G. *Inorg. Chem.* **1980**, *19*, 2854.

0020-1669/91/1330-3048$02.50/0

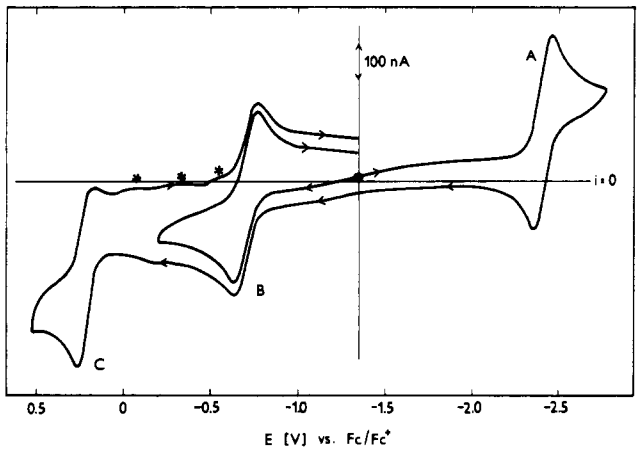

Figure 1. Cyclic voltammogram of $Bu_4N[Mn(CO)_3(DBCat)]$ in THF containing 0.1 M Bu_4NPF_6 at a Pt-disk electrode (scan rate 100 mV/s). Two independent scans (one positive, one negative) start from the point ●. The vertical line denotes the starting potential.

step (polarographic limiting current equals that of known one-electron couples Fc/Fc^+ [23] and DBQ/DBSQ[25]). The reduction is electrochemically reversible as follows both from polarography [log $((i_d - i)/i)$ vs E affords a linear plot[24] with a slope of 74 mV (as compared[26] with a slope of 78 mV for the Fc/Fc^+ couple)] and from cyclic voltammetry[27] [ΔE_p = 110 mV at 100 mV/s (ΔE_p = 100 mV for Fc/Fc^+)[26]]. Reduction is less reversible at low temperature (~203 K), where ΔE_p = 200 mV at 100 mV/s (Fc/Fc^+: ΔE_p = 130 mV). The electrochemical reversibility is good evidence for the formation of $[Mn(CO)_3(DBCat)]^{2-}$ by a simple one-electron transfer that is not accompanied by any major structural change.[24]

The anodic peak observed on the reverse scan at the Pt-disk electrode is well developed, $i_c^A/i_a^A \simeq 1$ within the scan rate range 20–200 mV/s. The peak current ratio is also independent of complex concentration over the range from 10^{-4} to 2×10^{-3} M.

In order to investigate the spectroscopic properties of $[Mn(CO)_3(DBCat)]^{2-}$, a solution of $Bu_4N[Mn(CO)_3(DBCat)]$ was reduced electrochemically in DMF (10^{-1} M Bu_4NPF_6) either at the Hg-pool electrode or within an EPR or OTTLE (i.e. optically transparent thin-layer electrochemical) cell at a Pt and Au minigrid electrode, respectively. Chemical reduction using 1% sodium amalgam in THF has also been employed. Bulk electrolysis afforded a mixed anodic–cathodic wave at the potential of the original cathodic wave. However, its current was much lower owing to partial decomposition during the prolonged reduction. Also, reduction by Na/Hg led to only small yields of the dianion. On the other hand, the reduced solutions are quite stable in the absence of mercury or Na/Hg, provided that air is rigorously excluded, as was shown both by OTTLE and EPR experiments. It appears that further decomposition of the dianion occurs in the presence of mercury, either in the form of the pool electrode or that of the amalgam. This is in accord with the low value of the i_a^A/i_c^A ratio (0.6–0.8) exhibited by cyclic voltammetry at the hanging mercury drop electrode (HMDE).

The electron paramagnetic resonance spectrum of the reduced solution (Figure 2) occurs at g = 2.0022, and it is split into a sextet due to a ^{55}Mn ($I = {}^5/_2$) hyperfine splitting: a_{Mn} = 53.4 G (THF), 54.8 G (DMF). The large a_{Mn} value, the absence of any splitting due to ^1H nuclei at the DBDiox ligand, and the large and alterating line width point clearly to a Mn-centered radical.

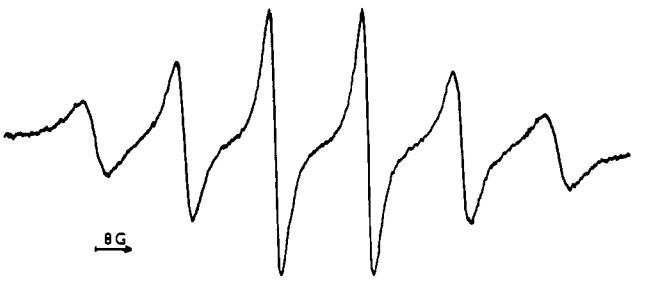

Figure 2. EPR spectrum of $[^*Mn(CO)_3(DBCat)]^{2-}$ in THF solution generated by reduction of 10^{-3} M $Bu_4N[Mn(CO)_3(DBCat)]$ with 1% Na/Hg for 5 min.

The infrared spectrum of the THF solution of $Bu_4N[Mn(CO)_3(DBCat)]$ reduced electrochemically within the IR OTTLE cell[28] at a gold minigrid electrode exhibits bands at 1890 (s), 1769 (m), and 1749 cm^{-1}, assigned to the $[Mn(CO)_3(DBCat)]^{2-}$ complex. When the starting solution was reduced by 1% Na/Hg, identical, albeit much less intense, IR bands were observed together with strong bands due to $Mn(CO)_5^-$ (1898, 1866 cm^{-1}), produced by the decomposition during the prolonged reduction with Na/Hg (vide supra). Reoxidation by a small amount of air diffusing slowly into the conventional IR cell regenerates the starting $[Mn(CO)_3(DBCat)]^-$ complex (1998, 1891 cm^{-1}).[22] This is good evidence that the bands at 1890, 1769, and 1749 cm^{-1} really belong to the reduced $[Mn(CO)_3(DBCat)]^{2-}$ complex. Its IR spectrum is quite comparable to those of $[Mn(CO)_3(PR_3)_2]^-$ species characterized by bands[29] in the range 1740–1780 cm^{-1}. A strong band at 1867 cm^{-1} was also found[29] for $[Mn(CO)_3(dppe)]^-$. The $[^*Mn(CO)_3(PR_3)_2]$ radicals show a characteristic IR band around 1855 cm^{-1} with a shoulder on its high-energy side.[30] Their spectra, however, were not followed in the 1700–1800 cm^{-1} range.[30]

Electronic Absorption Spectra. The reduction of $Bu_4N[Mn(CO)_3(DBCat)]$ has been performed in 10^{-1} M Bu_4NPF_6/THF solution at a gold minigrid electrode within an OTTLE cell. The bands of $[Mn(CO)_3(DBCat)]^-$ at 436 and 548 nm decrease, and less intense new bands at 404 nm (ϵ = 4500 M^{-1} cm^{-1}) and 536 nm (ϵ = 2500 M^{-1} cm^{-1}) appear isosbestically (λ_{iso} = 410 nm) during the reduction. Switching the potential to a value that is more positive than that of the reduction wave leads to the regeneration of the original monoanionic complex. Cycling the potential between negative and positive values may be repeated several times with only a minor decrease in the complex concentration. Obviously, the reduced species is rather stable and the $[Mn(CO)_3(DBCat)]^-/[Mn(CO)_3(DBCat)]^{2-}$ couple is chemically quite reversible.

On the other hand, the UV–vis spectrum of the THF solution of $Bu_4N[Mn(CO)_3(DBCat)]$ reduced by 1% Na/Hg is dominated by an intense band at 308 nm that belongs[25] to uncoordinated DBCat. (This was confirmed also by a $2e^-$ reduction of free *o*-DBQ followed spectroscopically in an OTTLE cell.) Introduction of a small amount of air to this solution leads to the regeneration of a very small amount of $[Mn(CO)_3(DBCat)]^-$ and to the appearance of an absorption in the red region (650–800 nm) that is typical[25] of free DBSQ. These species are obviously formed by oxidation of residual $[Mn(CO)_3(DBCat)]^{2-}$ and of free DBCat, respectively. [The EPR spectrum of such an air-oxidized solution exhibits only a signal due to an uncoordinated *o*-DBSQ (doublet, a_H = 3.3 G) and additional splitting due to the protons of the *C5-tert*-butyl group (0.25 G), confirming the above UV–vis results.]

In summary, the $[Mn(CO)_3(DBCat)]^-$ complex may be reduced electrochemically and chemically to give the rather stable $17e^-$ Mn-centered radical $[^*Mn(CO)_3(DBCat)]^{2-}$. This compound undergoes only slow decomposition. In the presence of Hg-con-

(24) Vlček, A. A. *Prog. Inorg. Chem.* **1963**, *5*, 211–384.
(25) Stallings, M. D.; Morrison, M. M.; Sawyer, D. T. *Inorg. Chem.* **1981**, *20*, 2655.
(26) Electrochemical reversibility of all electrode processes of $[Mn(CO)_3(DBCat)]^-$ was compared with that of the Fc/Fc^+ couple in the same solution to account for effects such as uncompensated *iR* drop, electrode passivation, etc.
(27) Brown, E. R.; Sandifer, J. R. *Physical Methods in Chemistry*, 2nd ed.; Rossiter, B. W., Hamilton, J. F., Eds.; Electrochemical Methods, Vol. 11; Wiley-Interscience: New York, 1986; pp 273–432.
(28) Krejčík, M.; Daněk, M.; Hartl, F. *J. Electroanal. Chem. Interfacial Electrochem.*, in press.
(29) Kuchynka, D. J.; Amatore, C.; Kochi, J. K. *J. Organomet. Chem.* **1987**, *328*, 133.
(30) McCullen, S. B.; Brown, T. L. *J. Am. Chem. Soc.* **1982**, *104*, 7496.

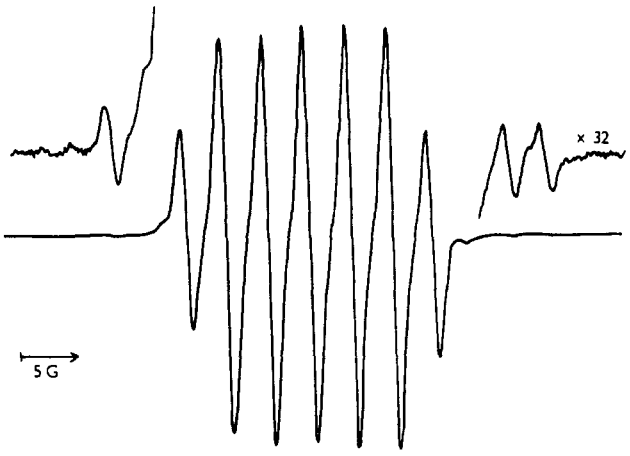

Figure 3. EPR spectrum of a $[Mn(CO)_3(THF)(DBSQ)]$ complex obtained by an in situ electrochemical oxidation of the THF (0.1 M Bu_4NPF_6) solution on a Pt-mesh electrode within a flat EPR cell. The broader weak signal, observable upon magnification, belongs to $[Mn(CO)_4(DBSQ)]$. It is absent after chemical ($FcBF_4$) or bulk electrochemical oxidations.

taining reducing agents (1% Na/Hg for 3 h, exhaustive electrolysis for 1.5 h at a Hg pool), $Mn(CO)_5^-$ and DBCat are formed as final products.

B. Oxidation. The oxidation of $[Mn(CO)_3(DBCat)]^-$ occurs in two successive one-electron steps in both coordinating (THF) and noncoordinating (CH_2Cl_2) solvents. However, the chemical reactivities of the primary oxidation products are quite different in these two solvents.

The final products of the first oxidation step were characterized spectroscopically in both solvents. Generally, the same spectroscopic results were obtained regardless of the method used for the oxidation of $[Mn(CO)_3(DBCat)]^-$. Treatment with ferrocinium cation ($FcBF_4$), bulk electrolysis at the mercury-pool electrode, or in situ electrolysis at Au or Pt minigrid electrodes inside the OTTLE or EPR cells, respectively, were employed to oxidize $[Mn(CO)_3(DBCat)]^-$.

Electron Paramagnetic Resonance. The oxidized THF solution of either the Bu_4N^+ or PPN^+ salt of $[Mn(CO)_3(DBCat)]^-$ exhibits the typical seven-line spectrum[31-33] of the $[Mn(CO)_3(THF)(DBSQ)]$ complex (Figure 3) (g = 2.0044, a_{Mn} = 3.7 G, a_H = 3.5 G, $a_{t\text{-}Bu}$ = 0.26 G)[34] whose intensity does not decay appreciably with time. In some spectra, especially when the oxidation was carried out by an in situ electrolysis within the flat EPR cell, a very weak signal of $[Mn(CO)_4(DBSQ)]$ (g = 2.0033, a_{Mn} = 7.0 G, a_H = 3.4 G) is present as a very small "satellite" to the much more intense spectrum of the $[Mn(CO)_3(THF)DBSQ)]$ complex (Figure 3).

In CH_2Cl_2, the EPR spectrum of the oxidized solution exhibits an intense $[Mn(CO)_4(DBSQ)]$ signal[33] (sextet of doublets, a_{Mn} = 6.9 G, a_H = 3.1 G) accompanied by a smaller signal of another, unidentified, radical at a similar g value. When the oxidation was carried out in CH_2Cl_2 solution saturated with CO at atmospheric pressure, the foreign EPR signal was no longer present and the spectrum of $[Mn(CO)_4(DBSQ)]$ was observed exclusively.

Contrary to $[Mn(CO)_3(THF)DBSQ)]$, $[Mn(CO)_4(DBSQ)]$ is not thermally stable and it undergoes a slow decomposition in Ar-saturated solution to an EPR-inactive species. However, it is stable under CO atmosphere.

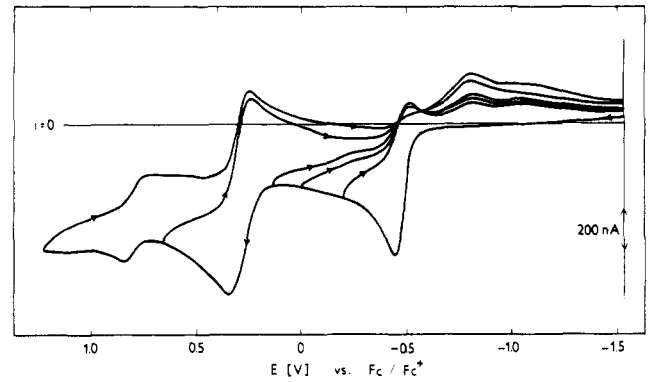

Figure 4. Cyclic voltammogram of $Bu_4N[Mn(CO)_3(DBCat)]$ in argon-saturated CH_2Cl_2 (0.1 M Bu_4NPF_6), with a scan rate of 50 mV/s, at a Pt-disk electrode. The vertical line denotes the starting potential.

The EPR experiments clearly show that the final products of the one-electron oxidations of $[Mn(CO)_3(DBCat)]^-$ in THF and CH_2Cl_2 are $[Mn(CO)_3(THF)(DBSQ)]$ and $[Mn(CO)_4(DBSQ)]$ complexes, respectively. The oxidation is obviously localized at the coordinated DBCat ligand, and in THF, it is accompanied by rapid solvent coordination. In relatively noncoordinating CH_2Cl_2, CO ligand disproportionation of the tricarbonyl to the tetracarbonyl species takes place. Interestingly, CO disproportionation was observed to occur to a small extent even in THF. This was particularly true for in situ electrolysis when the local concentration of the primary oxidation product at the electrode surface was relatively high, making the bimolecular CO disproportionation more competitive with solvent coordination.

Infrared spectra of the oxidized solutions of either the Bu_4N^+ or PPN^+ salt of $[Mn(CO)_3(DBCat)]^-$ in both THF and CH_2Cl_2 fully confirmed the EPR results. The original bands of $[Mn(CO)_3(DBCat)]^-$ at 1998 and 1891 cm^{-1} completely disappeared upon the addition of $FcBF_4$. In THF, new bands at 2030 (s), 1934 (m), and 1924 (sh) cm^{-1}, which are typical[33] of $[Mn(CO)_3(THF)(DBSQ)]$, were formed. In the presence of PPh_3, the $[Mn(CO)_3(PPh_3)(DBSQ)]$ complex (2025 (s), 1945 (m), and 1916 (m) cm^{-1})[33] was produced. On the other hand, in CH_2Cl_2, bands at 2105 (w), 2029 (s), 2004 (m), and 1960 (m) cm^{-1} appeared in both Ar- and CO-saturated solutions. These bands are fully characteristic of the $[Mn(CO)_4(DBSQ)]$ complex.[33] No other CO-containing species was observed in the argon-saturated solution of $Bu_4N[Mn(CO)_3(DBCat)]$ oxidized by $FcBF_4$. Obviously, the second disproportionation product undergoes rapid loss of CO ligands.

Electronic Absorption Spectra. The $[Mn(CO)_3(THF)(DBSQ)]$ complex prepared in THF solution by the oxidation of $Bu_4N[Mn(CO)_3(DBCat)]$ with $FcBF_4$ exhibits an absorption spectrum with bands at 310 nm (ϵ = 9830 M^{-1} cm^{-1}), 356 nm (sh), 524 nm (ϵ = 2370 M^{-1} cm^{-1}), and 708 nm (ϵ = 1650 M^{-1} cm^{-1}). The bands in the visible region are less intense than those of the parent $[Mn(CO)_3(DBCat)]^-$, which occur[22] at 436 nm (ϵ = 6250 M^{-1} cm^{-1}) and 548 nm (ϵ = 8300 M^{-1} cm^{-1}). When the oxidation was carried out electrochemically in an OTTLE cell, the absorption spectra of $[Mn(CO)_3(THF)(DBSQ)]$ and $[Mn(CO)_3(DBCat)]^-$ were easily interconverted by switching the electrolytic potential. This clearly demonstrates the chemical reversibility of the $[Mn(CO)_3(DBCat)]^-/Mn(CO)_3(THF)(DBSQ)]$ system.

The UV-vis spectrum of a CH_2Cl_2 solution of $Bu_4N[Mn(CO)_3(DBCat)]$ oxidized by $FcBF_4$ under an Ar atmosphere exhibits a weak unresolved absorption in the 450–660-nm range due to $[Mn(CO)_4(DBSQ)]$.

Electrochemistry. The cyclic voltammogram of $[Mn(CO)_3(DBCat)]^-$ in an argon-saturated *noncoordinating* CH_2Cl_2 solution at a Pt-disk electrode exhibits two one-electron oxidation steps followed by a small anodic peak (Figure 4). The first (most negative) oxidation occurs at $E_{1/2}$ = −0.48 V vs Fc/Fc^+ and it is an electrochemically quasireversible process (ΔE_p = 80 mV at 50 mV/s and the slope of a log plot[24] of the polarographic wave is 82 mV as compared[26] with ΔE_p = 65 mV and a slope of 78 mV

(31) Abakumov, G. A.; Cherkasov, V. K.; Shalnova, K. G.; Teplova, I. A.; Razuvaev, G. A. *J. Organomet. Chem.* **1982**, *263*, 333.
(32) Vlček, A., Jr. *J. Organomet. Chem.* **1986**, *306*, 63.
(33) van der Graaf, T.; Stufkens, D. J.; Vlčhová, J.; Vlček, A., Jr. *J. Organomet. Chem.* **1990**, *401*, 305.
(34) The a_H and $a_{t\text{-}Bu}$ splitting constants of the DBSQ ligand correspond to the hydrogen atom bound at the C4 position and to the hydrogen atoms of the *t*-Bu group bound at C5 position of the semiquinone ring, respectively: Felix, C. C.; Sealy, R. C. *J. Am. Chem. Soc.* **1982**, *104*, 1555.

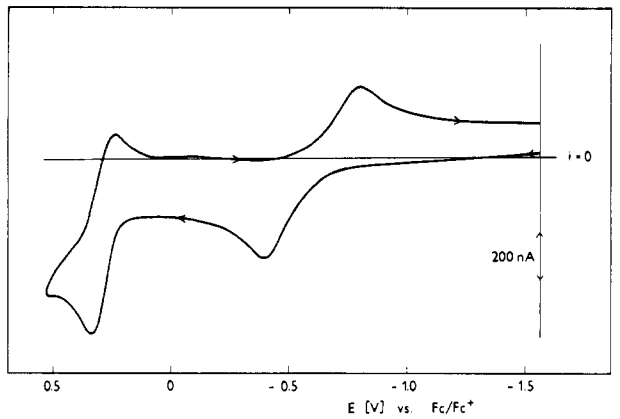

Figure 5. Cyclic voltammogram of $Bu_4N[Mn(CO)_3(DBCat)]$ in CO-saturated CH_2Cl_2 (0.1 M Bu_4NPF_6), with a scan rate of 100 mV/s, at a Pt-disk electrode. The vertical line denotes the starting potential.

found for Fc/Fc^+), the peak current being diffusion-controlled. On the reverse scan, the cathodic peak is well developed; however, the i_c/i_a ratio is significantly less than 1 even when the potential scan is reversed immediately after the first oxidation peak. The i_c/i_a ratio decreases as the scan reversal potential becomes more positive. Concomitantly, another reduction peak at[35] −0.82 V vs Fc/Fc^+ increases together with a smaller peak at approximately[35] −1.07 V (vs Fc/Fc^+). Keeping in mind that $[Mn(CO)_4(DBSQ)]$ is observed spectroscopically as the final product, one can interpret this behavior as follows: The electrochemical reversibility points to the formation of $[Mn(CO)_3(DBSQ)]$ as a primary electrode product. It undergoes a ligand-disproportionation reaction leading to $[Mn(CO)_4(DBSQ)]$, which is reducible at −0.82 V. The small peak at −1.07 V was tentatively assigned to the reduction of the second disproportionation product. These assignments are strongly supported by the cyclic voltammogram obtained in CO-saturated CH_2Cl_2 solution (Figure 5). In this case, the first anodic peak occurs at[35] −0.40 V. For the reverse scan, the cathodic peak corresponding to the reduction of $[Mn(CO)_3(DBSQ)]$ is missing and the only observable reduction is that of $[Mn(CO)_4(DBSQ)]$ at −0.80 V. Its peak current is equal to the anodic current if the scan is reversed just after the first anodic peak. The small cathodic peak at −1.07 V was not observed. These results show that the $[Mn(CO)_3(DBSQ)]$ primary electrode product takes up very rapidly and irreversibly a CO molecule, producing $[Mn(CO)_4(DBSQ)]$ without any side products. The $[Mn(CO)_4(DBSQ)]$ species is reducible more negatively at −0.80 V, rendering the first anodic peak chemically irreversible at 50 mV/s in CO-saturated solution.

The second, more positive, electrochemical oxidation occurs both in Ar- and CO-saturated CH_2Cl_2 solutions at +0.29 V vs Fc/Fc^+. It is an electrochemically quasireversible process (ΔE_p = 90 mV at 100 mV/s). The oxidation product is chemically stable, as i_c/i_a = 1 under both Ar and CO. This anodic peak was assigned by analogy with other dioxolene complexes to the oxidation of the coordinated DBSQ ligand in both $[Mn(CO)_3(DBSQ)]$ and $[Mn(CO)_4(DBSQ)]$ producing $[Mn(CO)_4(DBQ)]^+$. Occurrence of both these oxidations in a single wave is evidenced by the near-equivalence of the peak currents of the first and second anodic peaks and by the obvious broadness of the second anodic peak (Figure 4). Moreover, the DBSQ/DBQ ligand oxidation of the $[Mn(CO)_3(THF)DBSQ)]$ complex occurs at nearly the same potential (+0.23 V; vide infra), showing that the potential of the DBQ/DBSQ couple is almost independent of the other ligand L in the $[Mn(CO)_3(L)(DBSQ)]$ coordination sphere (L = CO, THF, vacancy), as expected for a strongly ligand-localized oxidation. (An alternative possibility is oxidation of the Mn(I) central atom. However, such a process may well be expected to be chemically and electrochemically irreversible due to the large inner-sphere reorganization involved and the expected instability of Mn(II)–carbonyl complexes.)

The third oxidation peak occurs in Ar-saturated CH_2Cl_2 solution at E_p = +0.86 V. This peak is absent under CO atmosphere. It was not studied further.

The cyclic voltammogram of $Bu_4N[Mn(CO)_3(DBCat)]$ in a *coordinating THF solvent* at a Pt-disk electrode or at the HMDE in the presence of 10^{-1} M Bu_4NPF_6 exhibits two successive oxidation peaks (Figure 1B,C) at −0.70 V (B) and +0.23 V (C) (vs Fc/Fc^+): The first oxidation (B) is electrochemically quasireversible (ΔE_p = 140 mV, compared[26] to 100 mV found for Fc/Fc^+) at a CV scan rate of 100 mV/s and almost reversible (log plot[24] slope of 78 mV as compared with 74 mV for Fc/Fc^+) on the polarographic time scale. The more positive oxidation (C) is fully reversible (ΔE_p = 100 mV at 100 mV/s). The current function $i_p v^{-1/2}$ is constant for both peaks B and C, proving that the currents are diffusion-controlled. The peak currents of oxidation peak C and of reduction peak A are the same whereas oxidation peak B is slightly lower (by some 20%) owing to the quasireversible character of the electrode process involved. On the reverse scan, cathodic peaks corresponding to both B and C are well developed. When the scan is reversed at the potential between peaks B and C, the i_c^B/i_a^B current ratio corresponding to peak B is 1 at v ranging from 20 to 200 mV/s, showing that the primary oxidation product is fully stable on the time scale of cyclic voltammetry. The product of the second oxidation (C) undergoes a decomposition, as $i_c^C/i_a^C \simeq 0.85$ at v = 100 mV/s. This partial decomposition of the second oxidation product leads to the decrease of i_c^B/i_a^B to about 0.8 when peak C is passed before reversing the potential scan (Figure 1). Small cathodic peaks that occur between cathodic peaks C and B on the reverse scan (Figure 1, ✱) probably belong to the decomposition products. At low temperature (203 K), the product of the second oxidation is stable on the CV time scale even at slow scan rates (20 mV/s): i_c^C/i_a^C = 1 and i_c^B/i_a^B = 1 regardless of the potential of the scan reversal, and the small peaks (✱) resulting from its decomposition disappear.

Spectroelectrochemically, $[Mn(CO)_3(THF)(DBSQ)]$ was detected as the only product of oxidation step B (vide supra). Observed electrochemical behavior can thus be interpreted as an electron transfer coupled with very rapid reversible THF coordination to the $[Mn(CO)_3(DBSQ)]$ primary electrode product. Consequently,[27] peak B appears both chemically and electrochemically reversible and it is shifted negatively with respect to the $[Mn(CO)_3(DBCat)]^-/[Mn(CO)_3(DBSQ)]$ couple observed in CH_2Cl_2 (−0.48 V; vide supra). However, THF is already present in the solvation sphere of $[Mn(CO)_3(DBCat)]^-$ at the very moment of the electrode reaction. Electrode process B should thus be viewed as a $\{[Mn(CO)_3(DBCat)]\cdots THF\}^-/[Mn(CO)_3(THF)DBSQ)]$ couple.

The second oxidation step (C) was again assigned to the oxidation of the DBSQ ligand producing $[Mn(CO)_3(THF)(DBQ)]^+$, which undergoes slow subsequent decomposition.

Discussion

The $[Mn(CO)_3(DBCat)]^-$ complex undergoes three one-electron redox steps that are electrochemically reversible or quasireversible and, in the case of the oxidations, coupled with other chemical reactions. The four-membered redox series is thus formulated as

$$[Mn(CO)_3(DBCat)]^{2-} \leftrightarrow [Mn(CO)_3(DBCat)]^-$$

$$[Mn(CO)_3(DBCat)]^- \leftrightarrow [Mn(CO)_3(DBSQ)]$$

$$[Mn(CO)_3(DBSQ)] + L \xrightarrow{\text{very fast}} [Mn(CO)_3(L)(DBSQ)]$$

$$L = THF, CO$$

$$[Mn(CO)_3(DBSQ)] \leftrightarrow [Mn(CO)_3(DBQ)]^+$$

$$[Mn(CO)_3(DBQ)]^+ + L \xrightarrow{\text{very fast}} [Mn(CO)_3(L)(DBQ)]^+$$

$$[Mn(CO)_3(L)(DBSQ)] \leftrightarrow [Mn(CO)_3(L)(DBQ)]^+$$

(35) The exact peak potential is somewhat dependent on the state of the electrode surface, which sometimes underwent passivation during the experiments. Reported values were obtained at a freshly polished Pt-disk electrode.

In the absence of a free ligand L (i.e. solutions in dry CH_2Cl_2), L is a CO molecule coming from another $[Mn(CO)_3(DBSQ)]$ or $[Mn(CO)_3(DBQ)]^+$ complex. The individual electron-transfer steps may be easily localized either at the redox-active DBDiox ligand or at the Mn central atom on the basis of the changes in the spectroscopic properties along the redox series.

The EPR spectra of the most reduced species $[Mn(CO)_3(DBCat)]^{2-}$ exhibit features typical of a metal-centered radical, specifically a large a_{Mn} value (53.4 G), comparable with that (40 G) of the one-electron-reduction product of $[Mn(CO)_4(S_2CNEt_2)]$.[36]

The IR spectrum of $[Mn(CO)_3(DBCat)]^{2-}$ exhibits very low $\nu(CO)$ frequencies, which resemble those[29] of the 18-electron Mn(-I) complexes $[Mn(CO)_3(PR_3)_2]^-$ more closely than they resemble those of 17-electron $[^{\bullet}Mn(CO)_3(PR_3)_2]$ species.[30] DBCat is, contrary to phosphines and phosphites, a very strong base[25] (i.e. strong σ-donor) and also a very strong π-donor.[3,18,22] Formally, the DBCat ligand in $[Mn(CO)_3(DBCat)]^{2-}$ donates more than the expected four electrons, strongly increasing the electron density on the Mn atom. The π-back-donation to the CO ligands is very extensive. Consequently, the $\nu(CO)$ frequencies are very low.

The chemical stability of $[Mn(CO)_3(DBCat)]^{2-}$ (lifetime of the order tens of minutes) is quite surprising for a Mn-centered 17-electron radical. Its dimerization is presumably sterically hindered by the bulky DBCat ligands.

The first oxidation step is localized on the DBCat ligand. The resulting $[Mn(CO)_3(L)(DBSQ)]$ species (L = THF, CO) are typical complexes of d^6-Mn(I) with a radical-anionic ligand.[31-33] They exhibit small a_{Mn} values, a_H splitting due to ring and *t*-Bu group protons of the DBSQ ligand, and a *g* factor that is very close to that of free DBSQ. The $\nu(CO)$ frequencies are higher than those of the parent $[Mn(CO)_3(DBCat)]^-$ and fall well within the range typical of other $[Mn(CO)_3L_3]^+$ complexes (L = acetone, py; $L_3 = \eta^5$-Cp^-).[22,33] The IR data clearly point to a significant decrease in the π-donor properties of the DBCat ligand upon its oxidation to the DBSQ radical anion.

The most interesting consequence of the DBCat → DBSQ ligand-centered oxidation is the profound change in the bonding properties of the central Mn atom. Although both $[Mn(CO)_3(DBCat)]^-$ and $[Mn(CO)_3(DBSQ)]$ are formally 5-coordinate 16-electron Mn(I) species, the Mn atom in the DBCat complex does not have any tendency to coordinate the sixth ligand,[22] whereas the DBSQ complex behaves as a strong Lewis acid. The DBCat → DBSQ oxidation is followed by a rapid addition of a Lewis base to saturate the coordination sphere. If no free base is present, the coordinative saturation is achieved by CO ligand disproportionation. This dramatic *increase in the coordinative ability of the central metal atom induced by the oxidation of the ligand* is caused by the loss of π-donation. The electron is removed from the Mn–DBCat π-bonding orbital, which is predominantly DBCat in character.[22] The decrease of the negative charge from DBCat to DBSQ stabilizes the DBDiox π orbital, thus increasing the energy gap with the empty metal d_π orbital. Consequently, π-donation and, especially, the delocalization of the Mn–DBDiox π-bonding are greatly diminished; the empty d_π orbital loses its π-character and is available for σ-bonding with the incoming sixth ligand. Such an expansion of the coordination sphere as a consequence of the DBCat ligand oxidation is a novel reaction type for metal–dioxolene complexes. In the isoelectronic complex $[Co^{III}(triphos)(DBCat)]$, substitution of DBSQ and, especially, substitution of DBQ are the reactions following the first and second oxidations, respectively.[11]

Surprisingly, the products of the second oxidation, $[Mn(CO)_3(L)(DBQ)]^+$ (L = THF, CO), are rather stable, especially in the presence of excess L.

The potentials of both DBQ/DBSQ and DBSQ/DBCat ligand couples in $[Mn(CO)_3(DBDiox)]^n$ ($n = +1, 0, -1$) are shifted by approximately 1.2 V positively with respect to those of free uncoordinated DBDiox species. This points to a strong stabilization of the reduced forms of the DBDiox ligand upon complexation. Potentials of both ligand-localized couples are shifted by nearly the same value. Obviously, the donor ability of the DBDiox ligand toward the $Mn(CO)_3^+$ structural unit decreases in the order DBCat > DBSQ > DBQ, the difference between DBCat and DBSQ being comparable with the difference between DBSQ and DBQ. The 1.2-V shift observed for $[Mn(CO)_3(DBDiox)]^n$ species is somewhat lower than shifts found for the oxomolybdenum(VI)–DBCat complex (1.8 V)[13] and, especially, for the isoelectronic $[Co(triphos)(DBDiox)]^n$ ($n = +1, +2, +3$) species, where shifts of +2.03 and 1.55 V were reported[11] for the DBCat/DBSQ and DBSQ/DBQ couples, respectively. It is apparent that the electron-rich DBCat ligand strongly favors high-valent electropositive metals. Although isoelectronic with $[Co(triphos)(DBCat)]^+$, $[Mn(CO)_3(DBCat)]^-$ contains the low-valent Mn(I) central atom, whose interaction with the DBCat ligand is weaker.

Conclusions

A four-membered redox series based on the DBDiox ligand bound to the $Mn(CO)_3^{+,0}$ structural unit exists: $[Mn(CO)_3(L)(DBQ)]^+$, $[Mn(CO)_3(L)(DBSQ)]$, $[Mn(CO)_3(DBCat)]^-$, and $[Mn(CO)_3(DBCat)]^{2-}$; L = THF, PPh_3, or CO. The $[Mn(CO)_3(DBSQ)]$ species exists only as an electrochemical intermediate observable by cyclic voltammetry. The neutral and dianionic members of this redox series are ligand-localized and metal-localized radicals, respectively. The change in the number of electrons between individual members of the redox series can be easily detected. The localized oxidation-state concept is fully suitable in this case. All complexes contain formally a Mn(I) central metal ion except for the dianion, which is a Mn(0) species.

Changes in the electron distribution are clearly reflected by the changes in spectroscopic properties along the redox series. The DBCat ligand is a very strong σ- and π-donor, which makes the Mn atom in $[Mn(CO)_3(DBCat)]^{-,2-}$ species more negatively charged than in other Mn(I) and Mn(0) complexes. On the other hand, π-bonding by the DBSQ ligand is negligible.[33]

Most interestingly, a dramatic increase in the Lewis acidity of the Mn atom is induced by the oxidation of the DBCat ligand in the $[Mn(CO)_3(DBCat)]^-$ complex. Its oxidation is followed by a very rapid coordination of a Lewis base to achieve a coordinative saturation.

Experimental Section

Materials. $PPN[Mn(CO)_3(DBCat)]\cdot 2C_6H_6$ and $Bu_4N[Mn(CO)_3(DBCat)]\cdot {}^1/_6C_6H_6$ were prepared according to ref 22. $FcBF_4$ was synthesized by a published method.[37] Its purity was checked electrochemically and spectroscopically. PPh_3 (Merck) was recrystallized from ethanol. Bu_4NPF_6 (Fluka) was dried in vacuo at 350 K for 10 h. Mercury used for bulk electrolyses and for the preparation of 1% Na/Hg was dried in vacuo at 305 K for 48 h. All solvents were freshly distilled under argon atmosphere directly into electrochemical or spectral cells or they were transferred by using a buret attached to a Schlenk tube. THF (Fluka) was distilled from a sodium–benzophenone mixture, CH_2Cl_2 (Fluka) from P_2O_5, and DMF (Lachema) from sodium anthracenide. All solutions were prepared and handled under an atmosphere of pure argon by using Schlenk techniques or on a vacuum line by using three or four freeze–pump–thaw cycles.

Instrumentation. The UV–vis absorption spectra were recorded on either a Carl-Zeiss-Jena M40 or a Hewlett Packard Model 8452A diode array spectrophotometer. A Philips PU9800 FTIR instrument was employed to record IR spectra. Matched 0.1-mm sealed KBr cells were used. EPR spectra were recorded on a Varian E4 X-band spectrometer. The *g* values were determined against a DPPH standard ($g = 2.0037 \pm 0.0002$). All electrochemical measurements were performed by using a PA4 polarographic analyzer (Laboratorní přístroje, Prague) with a three-electrode arrangement. The Pt-disk electrode (area 0.8 mm^2) was carefully polished with a 1-μm diamond paste before each CV measurement. A silver-wire quasireference electrode was employed. All potentials are thus referenced[23] to that of the Fc/Fc^+ couple. Fc was used as an internal standard also for the determination of electrochemical reversibility.[26] The UV–vis OTTLE cell was based on a design described by Gaš[38] and was modified to allow handling of very air- and moisture-

(36) Dessy, R. E.; Kornmann, R.; Smith, C.; Hayter, R. *J. Am. Chem. Soc.* **1968**, *90*, 2001.

(37) Hendrickson, D. N.; Sohn, Y. S.; Gray, H. B. *Inorg. Chem.* **1971**, *10*, 1559.

sensitive starting solutions. Our new design of the airtight IR OTTLE cell will be reported elsewhere.[28]

Registry No. THF, 109-99-9; $[Mn(CO)_3(DBCat)]^-$, 125665-75-0; $[Mn(CO)_3(DBCat)]^{2-}$, 125665-79-4; $[Mn(CO)_3(DBSQ)]$, 126388-40-7; $[Mn(CO)_3(DBQ)]^+$, 134109-78-7; $[Mn(CO)_3(THF)(DBQ)]^+$, 134078-40-3; $[Mn(CO)_3(PPh_3)(DBQ)]^+$, 134078-41-4; $[Mn(CO)_4(DBQ)]^+$, 134078-42-5; $[Mn(CO)_3(THF)(DBSQ)]$, 83951-62-6; $[Mn(CO)_3(PPh_3)(DBSQ)]$, 83970-81-4; $[Mn(CO)_4(DBSQ)]$, 83970-82-5; $[Mn(CO)_3(THF)(DBCat)]^-$, 134078-43-6; $[Mn(CO)_3(PPh_3)(DBCat)]^-$, 134078-44-7; $[Mn(CO)_4(DBCat)]^-$, 134078-45-8; $Bu_4N[Mn(CO)_3(DBCat)]$, 125665-77-2; PPh_3, 603-35-0; CO, 630-08-0; CH_2Cl_2, 75-09-2; Au, 7440-57-5; Pt, 7440-06-4; Hg, 7439-97-6.

(38) Gaš, B.; Klíma, J.; Záliš, S.; Vlček, A. A. *J. Electroanal. Chem. Interfacial Electrochem.* **1986**, *222*, 161.

Contribution from the Departament de Química, Universitat Autònoma de Barcelona, and Institut de Ciència de Materials, Campus de Bellaterra, Cerdanyola, 08193 Barcelona, Spain, and Department of Chemistry, University of Helsinki, Vuorikatu 20, SF-00100 Helsinki 10, Finland

Macrocycles Incorporating Sulfur and *nido*-Carborane Cages: Reactivity toward Nickel(II) and Palladium(II). Molecular Structures of $Pd\{7,8\text{-}\mu\text{-}(S(CH_2CH_2OCH_2CH_2OCH_2CH_2OCH_2CH_2)S)C_2B_9H_{10}\}_2$ and $Pd\{P(C_6H_5)_3\}Cl\{7,8\text{-}\mu\text{-}(SCH_2CH_2S)C_2B_9H_{10}\}$

Francesc Teixidor,*[†] Jaume Casabó,*[‡] Clara Viñas,[‡] Eustaquio Sanchez,[‡] Lluis Escriche,[‡] and Raikko Kivekäs[§]

Received June 12, 1990

The reactions of *exo*-dithio-7,8-dicarba-*nido*-undecaborate derivatives with Ni(II) and Pd(II) chlorides and phosphine chloride complexes are presented and discussed. Three different stoichiometries have been observed, $[MLCl_2]^-$, $[M_2L_2Cl_2]$, and $[ML_2]$. The capacity of these ligands to act as tricoordinating agents through the two sulfur atoms and a B(3)-H→M bond is introduced and discussed. A regularity in the value of the dihedral angle ω (planes defined by S-M-S and S-C_c-C_c-S) and the length of the exo-cluster chain has been observed. The shorter the exo-cluster chain is, the smaller the ω angle. The molecular structures of $Pd\{7,8\text{-}\mu\text{-}(S(CH_2CH_2OCH_2CH_2OCH_2CH_2OCH_2CH_2)S)C_2B_9H_{10}\}_2$ and $Pd\{P(C_6H_5)_3\}Cl\{7,8\text{-}\mu\text{-}(SCH_2CH_2S)C_2B_9H_{10}\}$ have been determined. The former crystallizes in space group $P2_1/c$ with 2 formula units per cell. The cell dimensions are a = 8.140 (2) Å, b = 20.083 (8) Å, c = 11.953 (3) Å, and β = 104.09 (2)°. The latter orystallizes in space group $P2_1/n$ with 4 formula units per cell. The cell dimensions are a = 13.424 (2) Å, b = 10.315 (2) Å, c = 20.008 (4) Å, and β = 90.83 (1)°.

Introduction

Thioethers are usually considered to be fairly poor ligands, not strongly bound to metals, and easily displaced by other ligands.[1] In their complexes, the "normal" coordination number of the metal ion is usually maintained, and metal-halogen coordination is dominant over metal-thioether.[2,3] Due to these characteristics most of the work about thioethers has been restricted to obtaining labile complexes, to studying pyramidal inversion at sulfur,[4-7] and searching for models for what they may reveal about structural changes accompanying oxidation and reduction of copper in metalloenzymes.[8,9] The poor ligand capacity of dithioethers has stimulated the study of all-sulfur multidentate ligands, mainly macrocycles. The polythioethers 1,4,7-trithiacyclononane (9S3),[10-13] 1,4,7,10,13,16-hexathiacyclooctadecane (18S6),[14-16] and their expanded homologues 12S3[17] and 24S6[18] have received considerable attention these last few years.

As opposed to normal dithioethers, here we wish to report on the high ligand capacity of another type of these compounds. These are derivatives of the 7,8-dicarba-*nido*-undecaborate anion, and their reactivity toward Ni(II) and Pd(II) metal ions is reported here altogether with the molecular structures of $Pd\{7,8\text{-}\mu\text{-}(S(CH_2CH_2OCH_2CH_2OCH_2CH_2OCH_2CH_2)S)C_2B_9H_{10}\}_2$ and $Pd\{P(C_6H_5)_3\}Cl\{7,8\text{-}\mu\text{-}(SCH_2CH_2S)C_2B_9H_{10}\}$. In these complexes metal-thioether coordination is dominant over metal-halogen coordination as opposed to normal dithioethers and some of them have been obtained by the diplacement of PPh_3 ligands, which is very uncommon in thioether chemistry. The exaltation of the ligand capacity has to be attributed to the carborane cage near the sulfur coordinating elements. Also, the capacity of these ligands to act as tricoordinating agents through the two sulfur atoms and a B-H→M bond is introduced. This type of bond has already been previously observed[19-23] but never with the boron

† Institut de Ciència de Materials.
‡ Universitat Autònoma de Barcelona.
§ University of Helsinki.

(1) Ainscough, E. W.; Brodie, A. M.; Palmer, K. C. *J. Chem. Soc., Dalton Trans.* **1976**, 2375.
(2) Lewason, W.; McAuliffe, C. A.; Murray, S. G. *J. Chem. Soc., Dalton Trans.* **1975**, 1566.
(3) Hartley, F. R.; Murray, S. G.; Levason, W.; Soutter, H. E.; McAuliffe, C. A. *Inorg. Chim. Acta* **1979**, *35*, 265.
(4) Abel, E. W.; Bhargava, S. K.; Kite, K.; Orell, K. G.; Sil, V.; Williams, B. L. *Polyhedron* **1982**, *3*, 289.
(5) Abel, E. W.; Orell, K. G.; Platt, A. W. G. *J. Chem. Soc., Dalton Trans.* **1983**, 2345.
(6) Boeré, R. T.; Willis, C. J. *Inorg. Chem.* **1985**, *24*, 1059.
(7) Gulliver, D. J.; Hale, A. L.; Levason, W.; Murray, S. G. *Inorg. Chim. Acta* **1983**, *69*, 25.
(8) Baker, E. N.; Norris, G. E. *J. Chem. Soc., Dalton Trans.* **1977**, 877.
(9) Olmstead, M. M.; Musker, W. K.; Kessler, R. M. *Inorg. Chem.* **1981**, *20*, 151.
(10) Bell, M. N.; Blake, A. J.; Schröder, M.; Küppers, H. J.; Wieghardt, K. *Angew. Chem., Int. Ed. Engl.* **1987**, *26*, 250.
(11) Rawle, S. C.; Admans, G. A.; Cooper, S. R. *J. Chem. Soc., Dalton Trans.* **1988**, 93.
(12) Hüppers, H. J.; Wieghardt, K.; Yi-Hung, T.; Krüger, C.; Nuber, B.; Weiss, J. *Angew. Chem., Int. Ed. Engl.* **1987**, *26*, 575.
(13) Wieghardt, K.; Küppers, H. J.; Raabe, E.; Krüger, C. *Angew. Chem., Int. Ed. Engl.* **1986**, *25*, 1101.
(14) Blake, A. J.; Gould, R. O.; Lavery, A. J.; Schröder, M. *Angew. Chem., Int. Ed. Engl.* **1986**, *25*, 274.
(15) Hartman, J. A. R.; Hintsa, E. J.; Cooper, S. R. *J. Am. Chem. Soc.* **1986**, *108*, 1208.
(16) Hartman, J. A. R.; Cooper, S. R. *J. Am. Chem. Soc.* **1986**, *108*, 1202.
(17) Rawle, S. C.; Sewell, T. J.; Cooper, S. R. *Inorg. Chem.* **1987**, *26*, 3769.
(18) Rawle, S. C.; Hartman, J. A. R.; Watkin, D. J.; Cooper, S. R. *J. Chem. Soc., Chem. Commun.* **1986**, 1083.
(19) Green, M.; Howard, J. A. K.; James, A. P.; Jelfs, A. P.; Nunn, C. M.; Stone, F. G. A. *J. Chem. Soc., Chem. Commun.* **1985**, 1778.
(20) Green, M.; Howard, J. A. K.; Jelfs, A. N. M.; Johnson, O.; Stone, F. G. A. *J. Chem. Soc., Dalton Trans.* **1987**, 73.
(21) Green, M.; Howard, J. A. K.; James, A. P.; Jelfs, A. N. M.; Nunn, C. M.; Stone, F. G. A. *J. Chem. Soc., Dalton Trans.* **1987**, 81.

0020-1669/91/1330-3053$02.50/0